Influence of the residual stresses on the crack deflection in ceramic laminates

Oldrich Sevecek[1,*], Michal Kotoul[1], Tomas Profant[1], Raul Bermejo[2]

[1] Institute of SMMB, Brno University of Technology, Brno 616 69, Czech Republic
[2] ISFK, Montanuniversitaet Leoben, Leoben 8700, Austria
* Corresponding author: sevecek@fme.vutbr.cz

Abstract The main goal of ceramic laminates designed with residual stresses is to increase the fracture energy of the system during fracture through energy dissipating mechanisms such as crack deflection or crack bifurcation. A computational tool based on Finite Fracture Mechanics (FFM) is implemented in this work to predict the propagation of cracks in ceramic laminates. The crack path is defined by the direction where maximum rate of the potential energy is released during fracture. Laminates studied here consist of two materials alternated in a layered structure designed with high compressive residual stresses, which are developed during cooling phase after sintering process. Different volume ratios of the material components are chosen in order to demonstrate the influence of the level of compressive residual stresses on the type of propagation (single crack deflection / crack bifurcation) and direction of the crack advance. Using the model a single crack deflection or crack bifurcation can be predicted for a given laminate. According to the calculations, the higher compressive stress in the layer is, the more the crack deflects from the straight direction and the more prone to the bifurcation. Results are in good agreement with experimental observations.

Keywords Ceramic laminates, Finite Fracture Mechanics, Crack propagation, Fracture criterion

1. Introduction

Ceramic laminates have become an alternative choice for the design of structural ceramics with improved fracture toughness and mechanical reliability. The brittle fracture of monolithic ceramics has been overcome by introducing layered architectures of different kind, i.e. geometry, composition of layers, weak interfaces, strong interfaces with residual stresses, etc. The main goal of such layered ceramics has been to increase the fracture energy of the system through energy dissipating mechanisms such as crack deflection, crack bifurcation, interface delamination, or crack shielding. Among the various laminate designs reported in literature, two main approaches regarding the fracture energy of the interfaces must be highlighted. On the one hand, laminates designed with weak interfaces have been reported to yield significant enhanced failure resistance through interface delamination [1-5]; the fracture of the first layer is followed by crack propagation along the interface, the so-called “graceful failure”, preventing the material from catastrophic failure. On the other hand, laminates designed with strong interfaces have shown significant crack growth resistance (R-curve) behavior through microstructural design (e.g. grain size, layer composition) [6-8] and/or due to the presence of compressive residual stresses, acting as a barrier (“*flaw tolerant*”) to crack propagation [2, 9-14].

The increase in fracture energy in these laminates is associated with energy dissipating mechanisms such as crack deflection/bifurcation phenomena, which act during crack propagation. The optimization of the layered design is based on the capability of the layers to deviate the crack from straight propagation. Experimental observations have shown the tendency of a crack to propagate with an angle through the compressive layer and even cause delamination of the interface [15] (see Fig. 1). It seems that the magnitude of compressive stresses may influence the angle of propagation

and subsequent delamination of the interface.

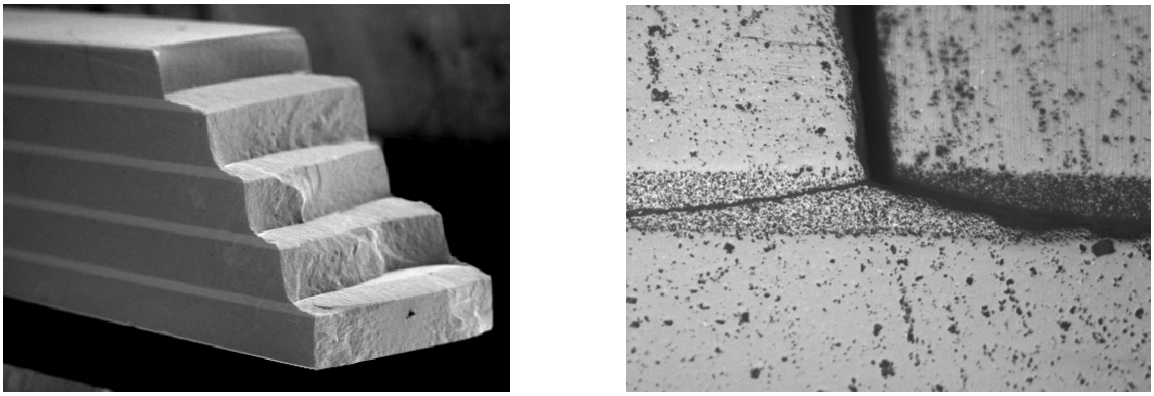

a) b)

Figure 1. a) Fracture of a ceramic laminate under flexural bending; bright layers have compressive residual stresses. b) Bifurcation of a crack entering the compressive layer of the laminate.

The prediction of the crack path upon loading in such layered systems should help in tailoring the design with maximal fracture energy. Methods based on energetic considerations are available which attempt to predict the behavior of a crack approaching the interface of dissimilar materials (see for instance Ref. [16]). However, the modeling of the propagation of an interface crack through layered architectures with residual stresses is still missing. A method which can be used to predict the conditions under which the crack deflects or bifurcates within the compressive layer is sought. In this work, a model based on the finite fracture mechanics approach is developed to interpret and predict the direction of propagation of a crack impinging an interface of a ceramic laminate designed with internal compressive residual stresses. The thermal strains in the layers occurring during sintering, which are responsible for the mechanical behavior of the laminate, are taken into account.

2. Model for crack path prediction in laminates

2.1. Material of study: loading configuration

A Finite Element analysis of a pre-cracked ceramic laminate specimen mechanically loaded in four-point bending was carried out. The thermal loading resulting from cooling down after sintering was also considered. The multilayer consists of a symmetric and periodic architecture with nine alternating layers of different thickness. In the initial state, a crack is introduced only in the first ATZ layer and impinges the first interface between ATZ and AMZ layer as depicted in Figure 2. Such laminate is subsequently subjected to the mechanical loading (4-point bend test). All the layers made of the same material, ATZ (alumina with 5% tetragonal zirconia), or AMZ (alumina with 30% monoclinic zirconia) have the same thickness, t_{ATZ} and t_{AMZ}, respectively. Table 1 gives the values of the constituent material properties employed in the calculations.

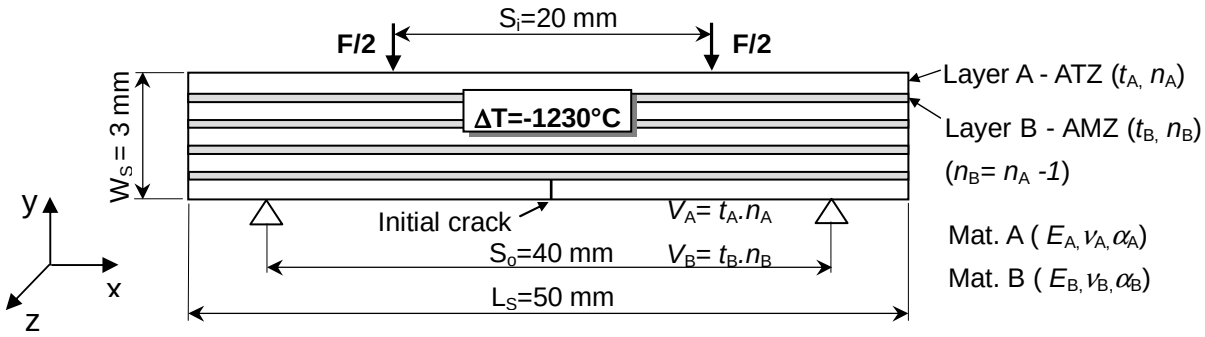

Figure 2. Schematic of the laminate of study with the applied boundary conditions (combined loading in 4-point bending flexure and residual stresses from sintering process). An initial crack is introduced in the first layer

Table 1. Young's modulus (E), Poisson's ratio (ν), Coefficient of Thermal Expansion (α), Flexural Strength (σ_f), Fracture Toughness (K_{Ic}) and Fracture Energy (G_c) of the layer materials

Material	E [GPa]	ν [-]	α x10^{-6} [K^{-1}]	σ_f [MPa]	K_{Ic} [MPa.$m^{1/2}$]	G_c [J/m^2]
ATZ	390±10	0.22	9.8±0.2	422±30	3.2±0.1	25±2
AMZ	280±10	0.22	8±0.2	90±20	2.6±0.1	23±2

In order to show the influence of the level of residual stresses on the propagation of the crack (i.e. deflection or bifurcation), three configurations with different volume ratio of the material components were considered and calculated. The total height of the laminate W_S was kept constant W_S =3mm and the thicknesses of the layers (t_{ATZ} and t_{AMZ}) were thus given by the chosen volume ratio – see (Table 2). The residual stresses corresponding to the chosen volume ratio configuration were calculated using the classical laminate theory by considering of ΔT = –1230°C (temperature between sintering and room temperature) and material properties given in the Table 1. The calculated residual stresses are listed in Table 2 as well.

Table 2. Layer thicknesses and corresponding residual stresses in the ATZ and AMZ layer for three different volume ratios of ATZ and AMZ material (W_S=const.=3mm)

V_{ATZ}/V_{AMZ} (t_{ATZ}/t_{AMZ})	t_{ATZ} [mm]	t_{AMZ} [mm]	$\sigma_{res,ATZ}$ [MPa]	$\sigma_{res,AMZ}$ [MPa]
2 (1.6)	0.400	0.250	+292	–585
5 (4.0)	0.500	0.125	+140	–695
8 (6.4)	0.533	0.083	+90	–730

2.2 Description of computational approach

In order to decide about the type of further crack propagation (single or double crack penetration) and/or about further crack propagation direction, a change of the potential energy $-\delta\Pi$ for the crack increments in all possible propagation directions has to be calculated. Direction and/or type of propagation is selected such that $\delta\Pi$ attains a maximum value (where maximum of energy is released by the fracture process). However one should note that the energy release rate (ERR) for

the crack terminating at the interface of two different materials is, for infinitesimally small crack increment, zero or infinite (depending on the singularity type). Thus the classical Griffith approach cannot be used. To bypass this problem, a theory of Finite Fracture Mechanics (FFM) can be employed – see e.g. references [20,21]. Infinitesimal crack increment is replaced by a finite crack increment for which the change of the potential energy can be calculated.

The essence of the FFM consists in the key assumption that crack propagation is a discontinuous process occurring in finite steps, rather than continuously and smoothly as in the traditional LEFM theory [20,22-24]. Mathematically, instead of using the differential form of the Griffith energy balance, the integral formulation of the Griffith criterion is applied. Such approach is of particular importance, for instance, in the case of a crack crossing thermo-elastically mismatched interfaces, where the energy release rate is either zero or infinite and, as a consequence, the differential approach fails. For example, if the crack penetrates from material layer 1 to layer 2, the concept of FFM states that the crack will follow the path which maximizes the additional energy ΔW_p released in the fracture process [24], as given by:

$$\Delta W_p = \delta\Pi_p - G_c^{(2)} a_p \,. \tag{1}$$

Here, $G_c^{(2)}$ is the toughness of the next layer to which crack penetrates, $\delta\Pi_p$ is a change of the potential energy between the original and new crack position, and a_p stands for an increment of the new crack.

Hereafter the concept of the Finite fracture mechanics is applied. Matched asymptotic expansions procedure, see e.g. [17-21], is used to derive the change of potential energy due to the perturbation caused by a single or branched crack extension of total length $a_p = a_b$ or a straight penetrating crack extension of length a_p (in several possible crack propagation directions φ_p – see Figure 3).

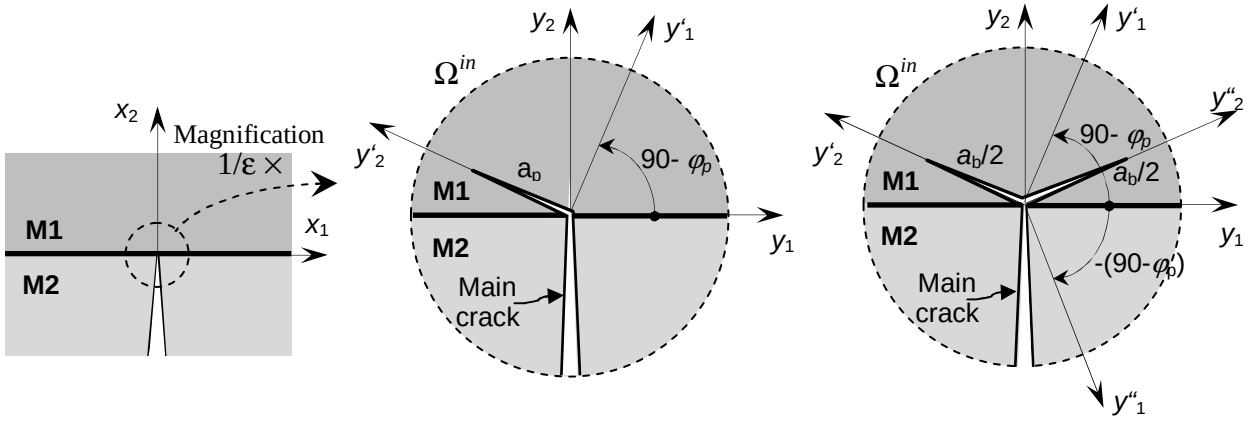

a) b) c)

Figure 3. Scheme of the a) crack terminating at the interface of M1 and M2, b) single crack deflection and c) crack bifurcation (branching) and local coordinate systems in the inner domain, where the crack extension length $a_p = a_b/2 + a_b/2 = 1$

The small perturbation parameter ε is defined as $\varepsilon=a_p/W_S<<1$, where W_S is the characteristic size of the specimen (e.g. specimen height). A second scale to the problem can be introduced, represented by the scaled-up coordinates $(y_1^{\varepsilon}, y_2^{\varepsilon})=(x_1/\varepsilon, x_2/\varepsilon)$ which provide a zoomed-in view into the region surrounding the crack, so-called inner domain Ω^{in} (see Figure 3).

The energy release rate is defined by:

$$G\left(a_{p(b)}\right)=\frac{1}{W_S}\lim_{\delta\varepsilon\to 0}\frac{\delta\Pi_{\varepsilon}-\delta\Pi_{\varepsilon+\delta\varepsilon}}{\delta\varepsilon}. \tag{2}$$

Assuming that the loading is constant during crack extension, the change of the potential energy $\delta\Pi_\varepsilon$ between the unperturbed state $\mathbf{U}^0$ (without the crack extension) and perturbed state $\mathbf{U}^{\varepsilon}$ (with the small finite crack extension) can be obtained from the asymptotic expansion with respect to a small parameter ε as:

$$\delta\Pi_\varepsilon=\Pi^0-\Pi^\varepsilon=\delta\Pi_\varepsilon^{(1)}+\delta\Pi_\varepsilon^{(2)}+....,\frac{\delta\Pi_\varepsilon^{(2)}}{\delta\Pi_\varepsilon^{(1)}}\to 0 \text{ for } \varepsilon\to 0 \text{ and } \delta_2<1, \tag{3}$$

where

$$\delta\Pi_\varepsilon^{(1)}=\frac{W_S^{2\delta_1}}{2}H_1^{\,2}K_{1p(b)}\left(\varphi_p\right)\varepsilon^{2\delta_1}+\frac{W_S^{\delta_1+\delta_2}}{2}H_1H_2\varepsilon^{\delta_1+\delta_2}\cdot\left(K'_{1p(b)}\left(\varphi_p\right)+K_{2p(b)}\left(\varphi_p\right)\right)+\frac{W_S^{2\delta_1}}{2}H_2^{\,2}K'_{2p(b)}\left(\varphi_p\right)\varepsilon^{2\delta_2}. \tag{4}$$

Where H_1 and H_2 are generalized stress intensity factors (GSIF) and δ_1, δ_2 are the corresponding singularity exponents ($\delta_1<\delta_2$) in the stress asymptotic expansion (see [20,21]). The coefficients $K_{1d(p)}$ and $K_{2d(p)}$ are computed in the inner domain Ω^{in}, which is unbounded for $\varepsilon\to 0$ but in the model employed in the finite element calculation, Ω^{in} is approximated by a circular region with radius R much larger than the crack extension length $a_{d(p)}$. On the circle boundary, the condition of the type $\mathbf{U}\big|_{\partial\Omega^{in}}=\rho^{\delta_1}\mathbf{u}_1(\theta)$ is prescribed. $K_{id(p)}$, $i=1,2$ are calculated using the path independent integral:

$$K_{ip(b)}=\int_\Gamma\left(\sigma_{kl}^h\left(\mathcal{V}_1^h(\rho,\theta)\right)n_l\rho^{\delta_i}u_{ik}(\theta)-\sigma_{kl}^s\left(\rho^{\delta_i}\mathbf{u}_i(\theta)\right)n_l\mathcal{V}_{1k}^h(\rho,\theta)\right)ds,\quad i=1,2 \tag{5}$$

Similarly, the coefficients $K'_{1d(p)}$, $K'_{2d(p)}$ are calculated in the inner domain whose remote boundary $\partial\Omega^{in}$ is subjected to the boundary condition $\mathbf{U}\big|_{\partial\Omega^{in}}=\rho^{\delta_2}\mathbf{u}_2(\theta)$

$$K'_{ip(b)}=\int_\Gamma\left(\sigma_{kl}^h\left(\mathcal{V}_2^h(\rho,\theta)\right)n_l\rho^{\delta_i}u_{ik}(\theta)-\sigma_{kl}^s\left(\rho^{\delta_i}\mathbf{u}_i(\theta)\right)n_l\mathcal{V}_{2k}^h(\rho,\theta)\right)ds,\quad i=1,2 \tag{6}$$

where $\sigma_{kl}^h, \mathcal{V}_i^h$, $i=1,2$ denotes FE approximation to the functions $\sigma_{kl}, \mathcal{V}_i$.

The second term of the change of the potential energy $\delta\Pi_\varepsilon^{(2)}$ depends on crack extension geometry. Two specific crack extension patterns are considered – crack bifurcation and crack deflection. For the case of the crack bifurcation $\delta\Pi_\varepsilon^{(2)}$ is given by:

$$\begin{aligned}\delta\Pi_{\varepsilon}^{(2)} = &-W_S^{1+\delta_1} H_1 \sigma_{xx}^{(M1)} \varepsilon^{\delta_1+1} \cos^2\varphi_p \left(\int_0^{1/2} \mathcal{V}_{1y_1'}(y')\,dy_2' + \int_0^{1/2} \mathcal{V}_{1y_1''}(y'')\,dy_2'' \right) + \\ &+ W_S^{1+\delta_1} H_1 \sigma_{xx}^{(M1)} \varepsilon^{\delta_1+1} \sin\varphi_p \cos\varphi_p \left(\int_0^{1/2} \mathcal{V}_{1y_2'}(y')\,dy_2' - \int_0^{1/2} \mathcal{V}_{1y_2''}(y'')\,dy_2'' \right) - \\ &- W_S^{1+\delta_2} H_2 \sigma_{xx}^{(M1)} \varepsilon^{\delta_2+1} \cos^2\varphi_p \left(\int_0^{1/2} \mathcal{V}_{2y_1'}(y')\,dy_2' + \int_0^{1/2} \mathcal{V}_{2y_1''}(y'')\,dy_2'' \right) + \\ &+ W_S^{1+\delta_2} H_2 \sigma_{xx}^{(M1)} \varepsilon^{\delta_2+1} \sin\varphi_p \cos\varphi_p \left(\int_0^{1/2} \mathcal{V}_{2y_2'}(y')\,dy_2' - \int_0^{1/2} \mathcal{V}_{2y_2''}(y'')\,dy_2'' \right) \gtrless 0,\end{aligned} \tag{7}$$

while for the case of single crack deflection $\delta\Pi_{\varepsilon}^{(2)}$ reads:

$$\begin{aligned}\delta\Pi_{\varepsilon}^{(2)} = &-W_S^{1+\delta_1} H_1 \sigma_{xx}^{(M1)} \varepsilon^{\delta_1+1} \cos^2\varphi_p \int_0^1 \mathcal{V}_{1y_1'}(y')\,dy_2' + W_S^{1+\delta_1} H_1 \sigma_{xx}^{(M1)} \varepsilon^{\delta_1+1} \sin\varphi_p \cos\varphi_p \int_0^1 \mathcal{V}_{1y_2'}(y')\,dy_2' - \\ &- W_S^{1+\delta_2} H_2 \sigma_{xx}^{(M1)} \varepsilon^{\delta_2+1} \cos^2\varphi_p \int_0^1 \mathcal{V}_{2y_1'}(y')\,dy_2' + W_S^{1+\delta_2} H_2 \sigma_{xx}^{(M1)} \varepsilon^{\delta_2+1} \sin\varphi_p \cos\varphi_p \int_0^1 \mathcal{V}_{2y_2'}(y')\,dy_2' \gtrless 0.\end{aligned} \tag{8}$$

The factors $K_{ip(b)}$ and the opening of the crack extension $\mathcal{V}_{1y_1'}, \mathcal{V}_{2y_1'}$ etc., are calculated by FEM on the inner domain – for methodology see e.g. references [20,21].
Note that GSIFs in Eqs. (4), (7) and (8) respectively are generally the sums of two contributions

$$H_1 = H_1^m + H_1^r, \quad H_2 = H_2^m + H_2^r, , \tag{9}$$

where H_i^m are due to pure flexural loading and H_i^r are due to pure thermal loading respectively. For calculation of GSIFs a two-state integral with FEM is employed - see [20,21].
Remark: If some of the GSIF H_1 or H_2 are close (or equal) to 0 (e.g. case of the crack perpendicular to the interface), then Eqs. (4), (7) and (8) will simplify significantly.

3. Results

The experimental observations (made by authors of [15]) shows that in case of laminates with higher volume ratios ($V_{ATZ}/V_{AMZ}>4$), the crack originated in the first ATZ layer does not stop at the interface, but arrests close behind the interface at a distance Δa (the distance Δa depends on the level of residual stresses). To explain this behavior, the thermal stress intensity factor for a wide range of crack lengths in ATZ layer and AMZ layer was calculated - see Figure 4. In terms of ERR the results are displayed in Figure 5. One can see that, for higher volume ratios, the crack has to be arrested close behind the interface since the SIF decreases rapidly by propagation in the compressive layer. At the distance of $\Delta a \cong 7\mu m$ (for V_{ATZ}/V_{AMZ} =8) and distance $\Delta a \cong 27\mu m$ (for V_{ATZ}/V_{AMZ} =5) the energy accumulated in the system is released and thus the crack is arrested. For subsequent propagation an additional mechanical loading is required. For the ratio V_{ATZ}/V_{AMZ} =2 the crack either arrests in much higher distance behind the interface or it propagates straight through the whole laminate (due to high tensile stresses in the first ATZ layer).

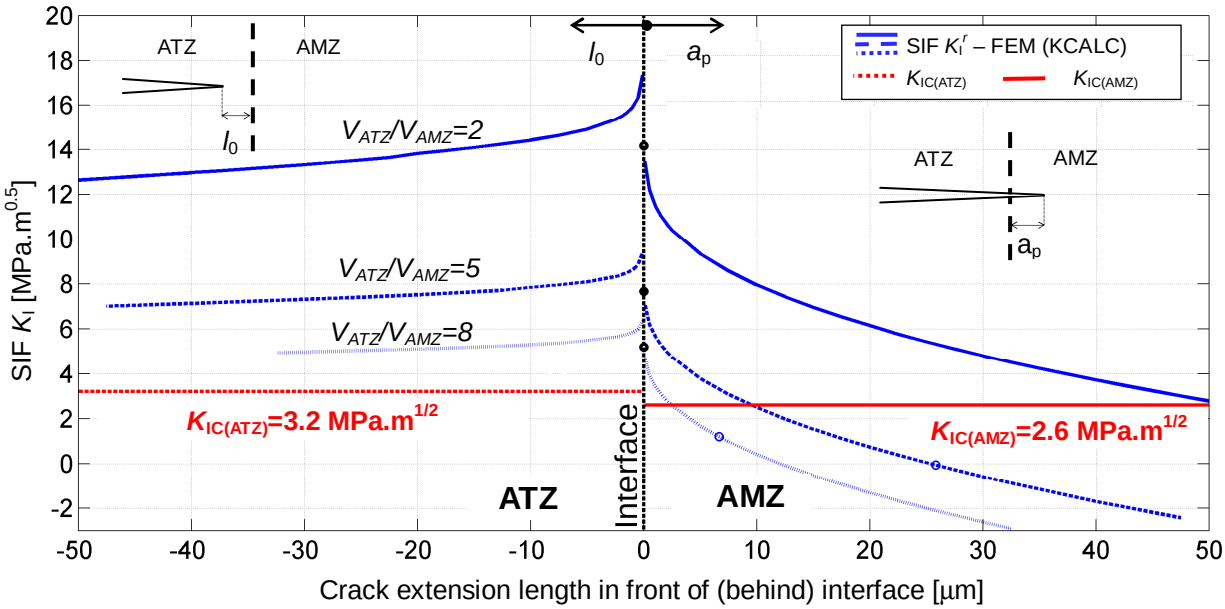

Figure 4. SIF K_I calculated for crack approaching interface and SIF K_I calculated for crack propagating straight in the second material. Laminate body was subjected to the thermal load ΔT=-1230°C. SIF K_I evaluated using ANSYS function KCALC.

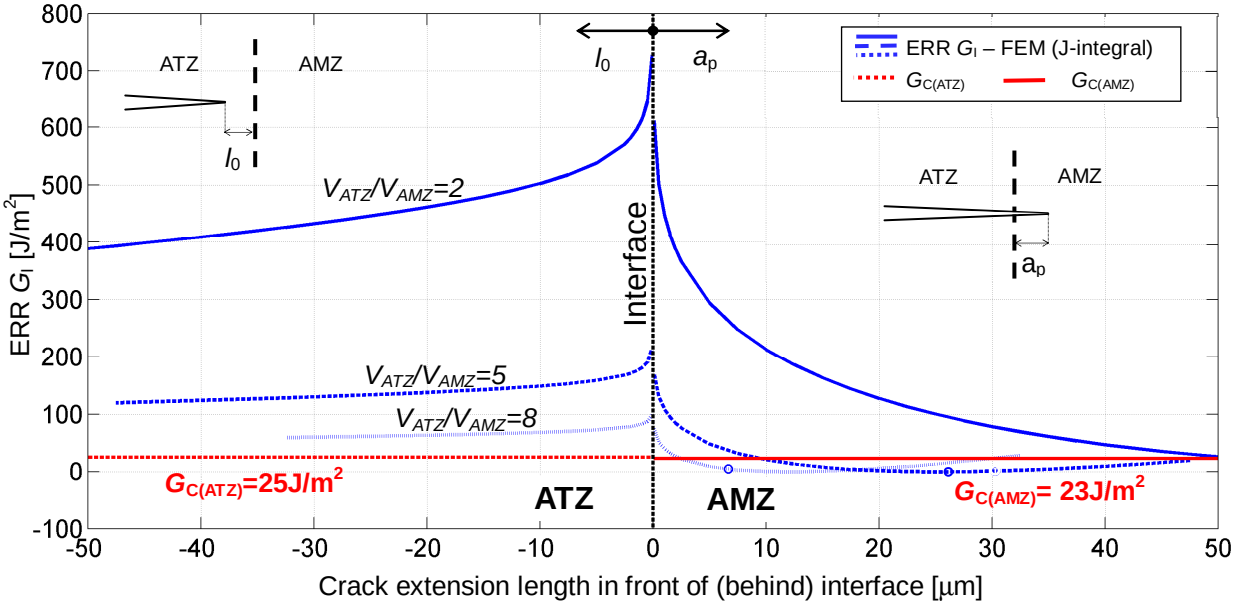

Figure 5. ERR G_I calculated for crack approaching interface and ERR G_I calculated for crack propagating straight in the second material. Laminate body was subjected to the thermal load ΔT=-1230°C. ERR G^r evaluated using the ANSYS function CINT (J-integral).

The values of the GSIFs characterizing the stress state at the crack tip for crack terminating at the interface of ATZ and AMZ layer are listed in Table 3. The GSIF for mechanical loading is calculated for a loading force of 10N. For higher forces it can be easily recalculated (due to its linear dependence on the applied load).

Table 3. Values of the GSIFs (crack terminating at the interface) for δ=0.46391, F=10N/mm, ΔT=-1230°C.

V_{ATZ}/V_{AMZ}	H^m [MPa.m$^{1-\delta}$]	H^r (ΔT) [MPa.m$^{1-\delta}$]	$\sigma_{xx}^{(AMZ)}$ (ΔT) [MPa]	$H=H^m+H^r$
2/1	0.10	2.92	-795	3.02
5/1	0.11	1.58	-795	1.69
8/1	0.11	1.07	-795	1.18

For the calculation of δΠ (Eqs. (2), (4), (7), (8)) for different propagation directions (including single penetration and bifurcation type of propagation) values of SIFs, corresponding to the state, when the crack is arrested behind the interface, were used – see Figure 5. Observe that SIF decreases rapidly with increasing length of crack extension behind the interface. In Figure 6 a), b) a ceramic laminate with volume ratio of laminate components V_{ATZ}/V_{AMZ}=8 is studied. Energetic condition for crack propagation (the additional energy $\Delta W \geq 0$ - see Eq. (1)) is satisfied for the loading force F≅100N. The referred figure shows a change in potential energy for case of single penetration and crack bifurcation (for $a_p=a_b$=25μm). One can see that crack bifurcation is a preferred propagation type in this case (due to higher change in potential energy).

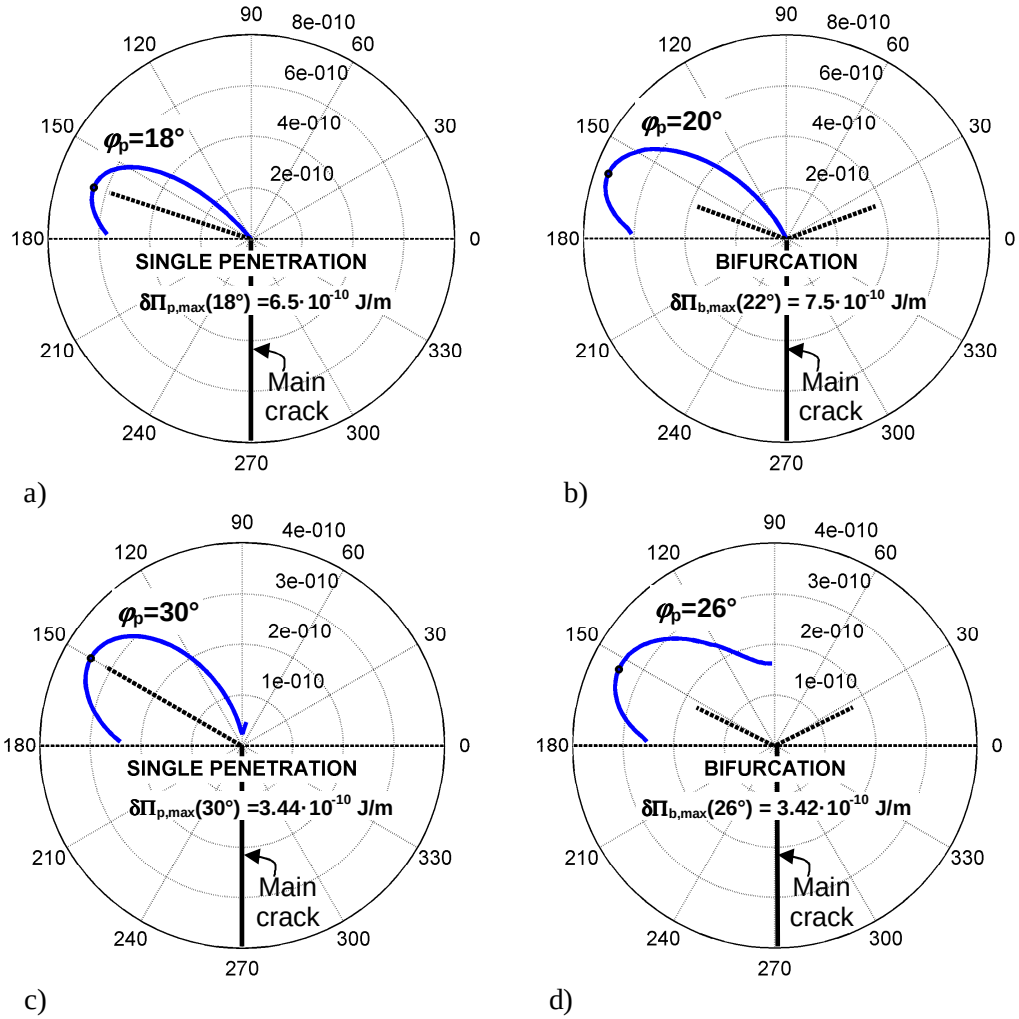

Figure 6. Variation of the change of the potential energy δΠ with the angle of the crack extension for a), b) volume ratio V_{ATZ}/V_{AMZ}=8 and c), d) V_{ATZ}/V_{AMZ}=5. For each volume ratio a case of single crack deflection - a), c) and case of the crack bifurcation - b), d) is calculated.

The same study was also made for ceramic laminate with V_{ATZ}/V_{AMZ}=5 - Figure 6 c), d) and here the critical loading force was estimated as F≅115N. In this case, a preferred propagation direction is starting to be a single deflection. For ratios V_{ATZ}/V_{AMZ}<5 only a single crack deflection is predicted as preferred propagation direction. In case of volume ratio V_{ATZ}/V_{AMZ}=2, the crack propagates almost straight, maximally with a slight deflection from the original direction (with no bifurcation phenomena).

4. Conclusions

The crack path in laminates is influenced by the magnitude and location of the compressive stresses in the internal layers. A semi-analytical model based on Finite Fracture Mechanics (FFM) theory was here developed to describe and predict the crack propagation in symmetric laminates consisting of alternated tensile–compressive layers built–up in a periodic architecture. In addition to the mechanical loading under flexural bending, a thermal loading associated with the thermal mismatch of the layers during sintering was also taken into account in the model. The fracture criterion was based on the calculation of the change of the potential energy $\delta\Pi$ for a finite crack increment length, starting from the tip of the original crack and advancing in several possible propagation directions (angle of crack propagation). From all theoretically possible crack paths, the change of the potential energy between unperturbed and perturbed state was evaluated. Direction and/or type of propagation were selected such that the change of $\delta\Pi$ would attain a maximum value.

In case of the low volume ratios (i.e. V_1/V_2= 1/1 – 4/1) single crack deflection (and in some cases straight crack propagation) is preferred with an angle lower than 20° (measured from the straight propagation). On the other hand, for relative high volume ratios, (i.e. V_1/V_2= 6/1 – 8/1), corresponding to high compressive residual stresses, crack bifurcation (i.e crack propagating simultaneously in two directions) is predicted by the model. Such behaviour is also in correspondence with the experimental observations.

Acknowledgements

The authors gratefully acknowledge a financial support through the project CZ.1.07/2.3.00/30.0005 of Brno University of Technology.

A financial support by the Austrian Federal Government (in particular from the Bundesministerium für Verkehr, Innovation und Technologie and the Bundesministerium für Wirtschaft und Arbeit) and the Styrian Provincial Government, represented by Österreichische Forschungsförderungs-gesellschaft mbH and by Steirische Wirtschaftsförderungsgesellschaft mbH, within the research activities of the K2 Competence Centre on “Integrated Research in Materials, Processing and Product Engineering”, operated by the Materials Center Leoben Forschung GmbH in the framework of the Austrian COMET Competence Centre Programme, is gratefully acknowledged as well.

References

[1] W.J. Clegg, K. Kendall, N.M. Alford, T.W. Button, J.D. Birchall, A Simple Way to Make Tough Ceramics. Nature, 347 (1990) 455-457.

[2] O. Prakash, P. Sarkar, P.S. Nicholson, Crack Deflection in Ceramic/Ceramic Laminates with Strong Interfaces. Journal of the American Ceramic Society, 78 (1995) 1125-1127.

[3] D.B. Marshall, P.E.D. Morgan, R.M. Housley, Debonding in multilayered composites of zirconia and $LaPO_4$. Journal of the american ceramic society, 80 (1997) 1677-1683.

[4] W.J. Clegg, Design of Ceramic Laminates for Strucutral Applications. Materials Science and Technology, 14 (1998) 486-495.

[5] H. Tomaszewski, H. Weglarz, A. Wajler, M. Boniecki, D. Kalinski, Multilayer ceramic composites with high failure resistance. J. of the Eur. Ceramic Society, 27 (2007) 1373-1377.

[6] D.B. Marshall, J.J. Ratto, F. Lange, Enhanced fracture toughness in layered microcomposites of Ce-ZrO_2 and Al_2O_3. J. Am. Ceram. Soc., 74 (1991) 2979-2987.

[7] J. Sanchez-Herencia, J. Moya, A. Tomsia, Microstructural design in alumina-alumina/zirconia layered composites. Scripta Materialia, 38 (1998) 1-5.

[8] R.J. Moon, K.J. Bowman, K.P. Trumble, J. Rödel, Fracture resistance curve behavior of multilayered alumina-zirconia composites produced by centrifugation. Acta Materialia, 49 (2001) 995-1003.

[9] R. Lakshminarayanan, D.K. Shetty, R.A. Cutler, Toughening of Layered Ceramic Composites with Residual Surface Compression. J. of the American Ceramic Society, 79 (1996) 79-87.

[10] M. Rao, J. Sanchez-Herencia, G. Beltz, R.M. McMeeking, F. Lange, Laminar ceramics that exhibit a threshold strength. Science, 286 (1999) 102-105.

[11] V.M. Sglavo, M. Paternoster, M. Bertoldi, Tailored Residual Stresses in High Reliability Alumina-Mullite Ceramic Laminates. J. of the Amer. Ceramic Society, 88 (2005) 2826-2832.

[12] M. Lugovy, V. Slyunyayev, N. Orlovskaya, G. Blugan, J. Kübler, M.H. Lewis, Apparent Fracture Toughness of Si_3N_4-Based Laminates with Residual Compressive or Tensile Stress in Surface Layers. Acta Materialia, 53 (2005) 289-296.

[13] R. Bermejo, Y. Torres, A.J. Sánchez-Herencia, C. Baudín, M. Anglada, L. Llanes, Residual stresses, strength and toughness of laminates with different layer thickness ratios. Acta Materialia, 54 (2006) 4745-4757.

[14] R. Bermejo, Y. Torres, C. Baudin, A.J. Sánchez-Herencia, J. Pascual, et al., Threshold strength evaluation on an Al_2O_3–ZrO_2 multilayered system. J Eur Ceram Soc, 27 (2007) 1443-1448.

[15] R. Bermejo, R. Danzer, High failure resistance layered ceramics using crack bifurcation and interface delamination as reinforcement mechanisms. Eng. Fract. Mech., 77 (2010) 2126-2135.

[16] M. He, J.W. Hutchinson, Crack Deflection at an Interface Between Dissimilar Elastic Materials. International Journal of Solids and Structures, 25 (1989) 1053-1067.

[17] E. Martin, D. Leguillon, C. Lacroix, A revisited criterion for crack deflection at an interface in a brittle bimaterial. Composites Sci. Technol., 61 (2001) 1671-1679.

[18] D. Leguillon, Strength or toughness? A criterion for crack onset at a notch. European Journal of Mechanics, A/Solids, 21 (2002) 61-72.

[19] L. Vu-Quoc, V. Tran, Singularity analysis and fracture energy-release rate for composites: Piecewise homogeneous-anisotropic materials. Comput. Methods Appl. Mech. Eng., 195 (2006) 5162-5197.

[20] M. Kotoul, O. Ševeček, T. Profant, Analysis of multiple cracks in thin coating on orthotropic substrate under mechanical and residual stresses. Eng. Fract. Mech., 77 (2010) 229-248.

[21] O. Ševeček, M. Kotoul, T. Profant, Effect of higher order asymptotic terms on the competition between crack penetration and debond at a bimaterial interface between aligned orthotropic materials. Eng. Fract. Mech., 80 (2012) 28-51.